Design Technique for Analog Temperature Compensation of Crystal Oscillators

Mark A. Haney

Thesis submitted to the Faculty of the Virginia Polytechnic Institute and State University
in partial fulfillment of the requirements for the degree of

Master of Science
In
Electrical Engineering

Dr. Dennis G. Sweeney
Dr. Charles W. Bostian
Dr. Ira Jacobs

Blacksburg, Virginia

Keywords: TCXO, Temperature Compensation, Crystal Oscillator

Abstract

For decades, the quartz crystal has been used for precise frequency control. In the increasingly popular field of wireless communications, available frequency spectrum is becoming very limited, and therefore regulatory agencies have imposed tight frequency stability requirements. There are generally two techniques for controlling the stability of a crystal oscillator with temperature variations of the environment. They are temperature control and temperature compensation.

Temperature control involves placing the sensitive components of an oscillator in a temperature stable chamber. Usually referred to as an oven-controlled crystal oscillator (OCXO), this technique can achieve very good stability over wide temperature ranges. Nevertheless, its use in miniature battery powered electronic devices is significantly limited by drawbacks such as cost, power consumption, and size.

Temperature compensation, on the other hand, entails using temperature dependent circuit elements to compensate for shifts in frequency due to changes in ambient temperature. A crystal oscillator that uses this frequency stabilization technique is referred to as a temperature-compensated crystal oscillator (TCXO). With little added cost, size, and power consumption, a TCXO is well suited for use in portable devices.

This paper presents the theory of temperature compensation, and a procedure for designing a TCXO and predicting its performance over temperature. The equivalent electrical circuit model and frequency stability characteristics for the AT-cut quartz crystal are developed. An oscillator circuit topology is introduced such that the crystal is operated in parallel resonance with an external capacitance, and equations are derived that express the frequency stability of the crystal oscillator as a function of the crystal's capacitive load. This relationship leads to the development of the theory of temperature compensation by a crystal's external load capacitance. An example of the TCXO design process is demonstrated with the aid of a MATLAB script.

Table of Contents

List of Figures

List of Equations

List of Tables

Chapter 1: Introduction

Crystal oscillators are the heartbeat of modern communication systems. For decades, the quartz crystal has been used for precise frequency control. Applications that require accurate frequency control include wireless transmitters, digital circuits, and time-based measurement instruments. In the increasingly popular field of wireless communications, available frequency spectrum is becoming very limited. Regulatory agencies have imposed tight restrictions on bandwidth and frequency stability. These requirements vary throughout the spectrum in accordance with the intended applications.

Many factors affect the frequency stability of an oscillator. These include variations in voltage, time, and temperature. Specifications for frequency stability are expressed as the amount of the divergence from the nominal operating frequency, usually in terms of a percentage or in parts per million (ppm).

There are generally two methods of controlling the instability of an oscillator due to temperature variations of its environment. The first is the method of temperature control. It involves the use of some kind of temperature stable chamber in which the sensitive components of the oscillator are placed. In the case of a crystal oscillator, the crystal is placed in a thermal oven that is held at a constant temperature. This circuit is called an oven-controlled crystal oscillator (OCXO). Very good stability over wide temperature ranges can be achieved. However, there are some disadvantages. The oven itself is usually a somewhat bulky unit that draws a considerable amount of current to maintain a constant temperature. This significantly restricts its use in miniature battery powered electronic devices. In addition, an oven-stabilized oscillator needs an initial warm-up period before it reaches a stable frequency. In the applications where the size, current draw, and warm-up period are tolerable, this approach to frequency stability is usually very desirable.

The second method is temperature compensation. This technique entails the use of some kind of temperature dependent circuitry to interact with the resonating components of the oscillator. A crystal oscillator that uses this frequency stabilization technique is referred to as a temperature-compensated crystal oscillator (TCXO). A TCXO can be implemented with a voltage-variable capacitor (varactor) circuit controlled by a temperature-dependent voltage (generated either digitally or by thermistor networks), or using specific temperature-dependent passive components to adjust the resonant frequency of the circuit. The advantages of a passive TCXO are: little added size to the overall circuit; little (if any) extra current draw; and minimum warm-up period (the amount of time an oscillator circuit requires for self heating effects to become uniform and constant). If the frequency control requirements for a particular design are not terribly stringent (i.e. frequency stability ~ ±2ppm over an operating temperature range from –20°C to +70°C), a temperature compensating circuit can be completely implemented using discrete analog temperature-sensitive components.

This paper presents the theory of temperature compensation, and a procedure for designing a TCXO and predicting its performance over temperature. First, the equivalent electrical circuit model and frequency stability characteristics for the AT-cut quartz crystal are developed, followed by a discussion on the theory of temperature compensation. Next, procedures for measuring a crystal's equivalent circuit parameters and frequency-temperature characteristics are described. A TCXO circuit topology is then introduced and equations are derived that express the frequency stability of the crystal oscillator as a function of the crystal's capacitive load. Finally, an example of the TCXO design process is demonstrated with the aid of a MATLAB script.

Chapter 2: Frequency-Temperature Characteristics

2.1 Basic Crystal Characterization

A quartz crystal is a mechanical resonator. It is constructed from a thin slab of quartz placed between two electrodes. Quartz is a piezoelectric material. When a mechanical force is applied to it, electric charges appear in a direction perpendicular to the force. Conversely, when an electric field is applied to the material, a mechanical deflection is produced in the quartz. If an alternating voltage is applied to the electrodes, the quartz will vibrate due to the alternating electric field induced across it. The amplitude of the vibration is a function of the frequency of the alternating electric field, becoming largest when the frequency is equal to the physical natural frequency of the crystal. The mechanical stresses of the vibrations in turn produce an oscillatory electric field, which controls the effective impedance between the two electrodes as a function of the excitation frequency. Quartz crystals typically have Q factors in the tens of thousands. [Frerking]

The key to understanding the frequency-dependent impedance of the quartz crystal is to represent it by an equivalent electrical circuit and analyze it using conventional filter theory. In order to describe the crystal by an equivalent circuit, a mechanical system and its electrical analog are needed. Figure 2.1 shows the equivalent electrical model of the crystal resonator. It is a mechanical vibrating system. The motional parameters of the crystal (inertia, stiffness, and internal losses) are represented by series inductance, capacitance, and resistance (L_m, C_m, and R_m). The capacitance formed by the electrodes of the crystal and the quartz dielectric is represented by the capacitor C_0 (the static capacitance). [Salt]

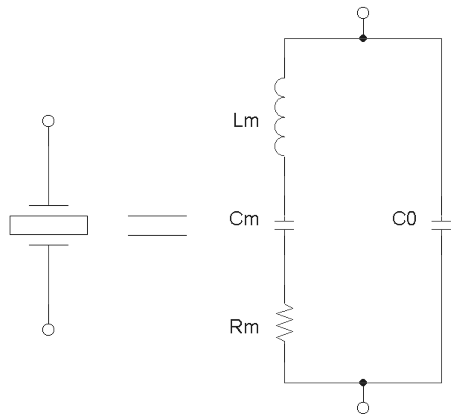

Figure 2.1: Equivalent circuit of a quartz crystal.

The impedance of the motional arm of the model can be defined as $Z_m = R_m + j\left(2\pi f L_m - \dfrac{1}{2\pi f C_m}\right)$. The impedance of the static capacitance is $Z_0 = j\dfrac{-1}{2\pi f C_0}$. The parallel combination of Z_m and Z_0 form the equivalent impedance between the electrodes as shown in Equation 2.1.

$$Z_{eq} = \frac{Z_0 Z_m}{Z_0 + Z_m} = \frac{\dfrac{-j}{2\pi f C_0}\left[R_m + j\left(2\pi f L_m - \dfrac{1}{2\pi f C_m}\right)\right]}{R_m + j\left(2\pi f L_m - \dfrac{1}{2\pi f C_m} - \dfrac{1}{2\pi f C_0}\right)}$$

Equation 2.1: Impedance of a quartz crystal.

By algebraic manipulation, Equation 2.1 can be re-written in a form (Equation 2.2) that lends itself to easy analysis.

$$Z_{eq} = \left(\frac{2\pi f L_m - \frac{1}{2\pi f C_m}}{2\pi f C_0 R_m} \right) \times \frac{1 + j\left[\left(\frac{-R_m}{2\pi f C_0} \right) \left(\frac{2\pi f C_0}{2\pi f L_m - \frac{1}{2\pi f C_m}} \right) \right]}{1 + j\left[\frac{2\pi f L_m}{R_m} - \frac{1}{R_m 2\pi f C_m} - \frac{1}{R_m 2\pi f C_0} \right]}$$

Equation 2.2: Impedance of a quartz crystal in analysis friendly form.

Resonance occurs at a frequency when Z_{eq} is purely real. From Equation 2.2, Z_{eq} is only real when the imaginary part of the numerator is equal to the imaginary part of the denominator as shown in Equation 2.3:

$$\left(\frac{-R_m}{2\pi f C_0} \right) \left(\frac{2\pi f C_0}{2\pi f L_m - \frac{1}{2\pi f C_m}} \right) = \frac{2\pi f L_m}{R_m} - \frac{1}{R_m 2\pi f C_m} - \frac{1}{R_m 2\pi f C_0}$$

Equation 2.3: Condition for resonance.

Using the quadratic formula to solve for *f*, Equation 2.4 is derived. [Frerking]

$$f = \frac{1}{2\pi} \sqrt{ \left(\frac{1}{L_m C_m} + \frac{1}{2 L_m C_0} - \frac{R_m^2}{2 L_m^2} \right) \pm \sqrt{ \left(\frac{1}{2 L_m C_0} - \frac{R_m^2}{2 L_m^2} \right)^2 - \frac{R_m^2}{L_m^3 C_m} } }$$

Equation 2.4: Solution for resonant frequencies of a quartz crystal.

For any practical quartz crystal, R_m is usually less than 100Ω, C_m is on the order of 10^{-15} F, L_m is on the order of 10^{-3} H, and C_0 is typically a few pico-Farads. The following assumption (Equation 2.5) is used to simplify Equation 2.4. [Frerking]

$$\left(\frac{1}{2L_mC_0}-\frac{R_m^2}{2L_m^2}\right)^2 >> \frac{R_m^2}{L_m^3C_m} \Rightarrow \sqrt{\left(\frac{1}{2L_mC_0}-\frac{R_m^2}{2L_m^2}\right)^2-\frac{R_m^2}{L_m^3C_m}} \cong \left(\frac{1}{2L_mC_0}-\frac{R_m^2}{2L_m^2}\right)$$

Equation 2.5: Assumption used for simplification of resonant frequency solution.

This leads to a simplified approximate solution for a quartz crystal's resonant frequency (Equation 2.6). [Frerking]

$$f \cong \frac{1}{2\pi}\sqrt{\left(\frac{1}{L_mC_m}+\frac{1}{2L_mC_0}-\frac{R_m^2}{2L_m^2}\right)\pm\left(\frac{1}{2L_mC_0}-\frac{R_m^2}{2L_m^2}\right)}$$

Equation 2.6: Approximate resonant frequency solution.

There are two solutions for Equation 2.6. The first solution, obtained by using the minus sign, is denoted the series resonant frequency (Equation 2.7). The second solution, obtained by using the plus sign, is denoted the antiresonant (or parallel resonant) frequency (Equation 2.8). [Frerking]

$$f_s \cong \frac{1}{2\pi}\sqrt{\frac{1}{L_mC_m}}$$

Equation 2.7: Series resonant frequency.

$$f_a \cong \frac{1}{2\pi}\sqrt{\frac{1}{L_mC_m}+\frac{1}{L_mC_0}-\frac{R_m^2}{L_m^2}}$$

Equation 2.8: Antiresonant frequency.

Again, for any practical quartz crystal, the equivalent circuit parameters have typical values as mentioned previously. Therefore, a valid approximation that $\frac{1}{L_mC_0} >> \frac{R_m^2}{L_m^2}$ is used to simplify the antiresonant frequency to Equation 2.9. [Frerking]

$$f_a \cong \frac{1}{2\pi}\sqrt{\frac{1}{L_m C_m}+\frac{1}{L_m C_0}} \cong \frac{1}{2\pi}\sqrt{\frac{1}{L_m C_m}}\sqrt{1+\frac{C_m}{C_0}}$$

Equation 2.9: Approximation for antiresonant frequency.

Since $\frac{C_m}{C_0} << 1$, the binomial approximation $(1+x)^n \cong 1+nx$ is used to further simplify Equation 2.9. This results in Equation 2.10. [Frerking]

$$f_a \cong \frac{1}{2\pi}\sqrt{\frac{1}{L_m C_m}}\left(1+\frac{C_m}{2C_0}\right) \cong f_s\left(1+\frac{C_m}{2C_0}\right)$$

Equation 2.10: Simplified approximation for antiresonant frequency.

The series resonant frequency is the natural frequency of the motional arm of the crystal. The antiresonant (or parallel resonant) frequency is the frequency at which the motional arm reactance resonates with the static capacitance, C_0. At frequencies between f_s and f_a, the impedance of the crystal appears inductive. At frequencies just below f_s or just above f_a, the crystal looks capacitive. Figure 2.2 shows a graph of reactance versus frequency for a crystal (C_m=6.1x10^{-15}F, L_m=25.3mH, R_m=25Ω, C_0=2.0pF) that has a series resonant frequency of approximately 12.798913 MHz.

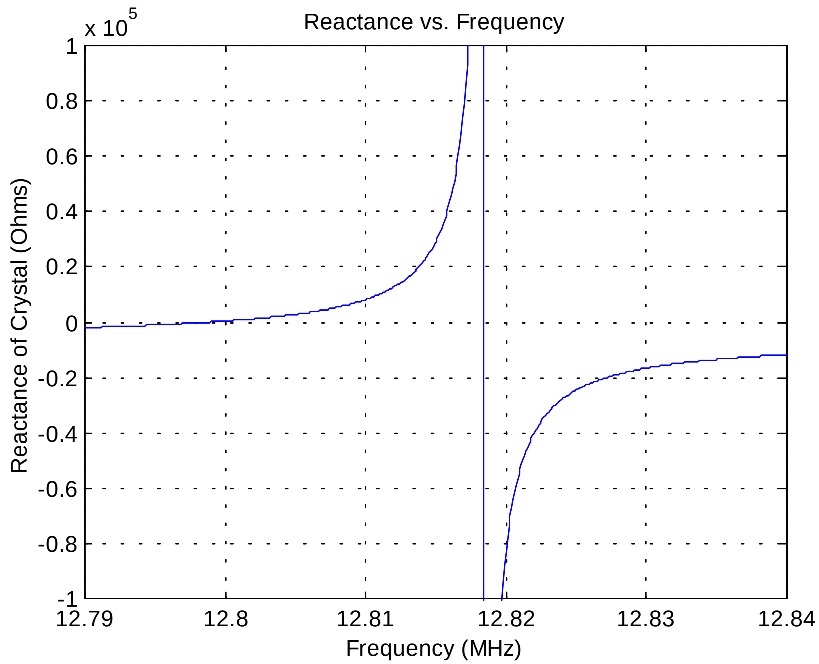

Figure 2.2: Graph of a crystal's reactance vs. frequency.

2.2 Crystal Temperature Characteristics

The most commonly used type of crystal is the AT-cut crystal, where the quartz blank is in the form of a thin plate cut at a nominal angle, θ_0, of about 35.25° to the optical axis of the crystal. The frequency-temperature characteristics of the crystal can be controlled by small variations in the angle of the cut. [Salt]

The AT-cut crystal has a frequency-temperature characteristic described by a cubic function of the form given in Equation 2.11 [Frerking].

$$\frac{\Delta f}{f_0} = A_1(T - T_0) + A_2(T - T_0)^2 + A_3(T - T_0)^3$$

Equation 2.11: Frequency-temperature relationship of AT-cut crystals.

The value $\frac{\Delta f}{f_0}$ refers to the relative frequency change as a function of the temperature. The coefficients A_1, A_2, and A_3 depend on physical properties of the crystal including the angle of the cut, ratio of dimensions, order of overtone, shape of plate, and type of mounting. [Bechmann]

Within small angle ranges about the nominal angle for the AT-cut, the coefficients can be expressed as linear functions of the angle $\Delta\theta$, measured in degrees from the angle θ_0. [Salt]

A typical AT-cut family of frequency-temperature characteristic curves is shown in Figure 2.3. These curves represent three different angles of the cut. This illustrates the dependence the frequency stability of the crystal has on the angle of the cut.

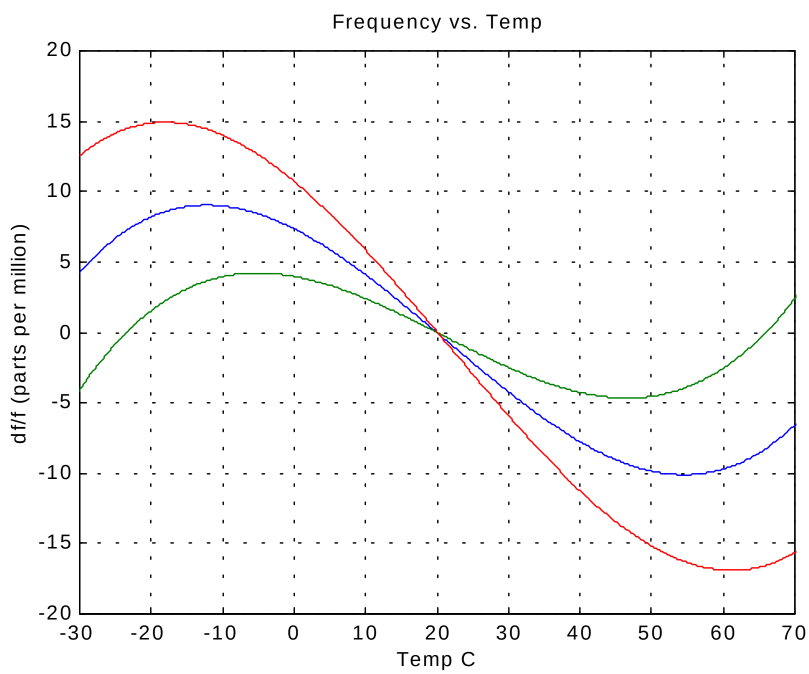

Figure 2.3: Typical frequency-temperature curves for AT-cut crystals.

Chapter 3: Theory of Temperature Compensation

3.1 Crystal with a Capacitive Load

Many oscillator circuits make use of a capacitive load, C_L, in series or parallel with the crystal. The presence of the load capacitance pulls the frequency of the crystal by an amount depending upon the value of C_L and the values of C_m and C_0.

When a crystal is operated as a parallel resonant circuit, an external capacitive load is presented in parallel to the crystal to pull it to the desired frequency of resonance. The capacitive load, C_L, and the crystal's static capacitance, C_0, are effectively in parallel, resulting in a combined parallel resonant frequency, f_L. By modifying C_0 in Equation 2.10, f_L can be expressed as shown in Equation 3.1.

$$f_L = f_s\left(1+\frac{C_m}{2(C_0+C_L)}\right)$$

Equation 3.1: Parallel resonant frequency of a crystal due to an external capacitive load.

The term Δf_{sL} can be used to represent $f_L - f_s$ (the offset in resonant frequency from f_s due to C_L). Equation 3.1 can be re-written in the form of Equation 3.2.

$$\frac{\Delta f_{sL}}{f_s} = \frac{f_L - f_s}{f_s} = \frac{C_m}{2(C_0+C_L)}$$

Equation 3.2: Parallel resonant frequency expressed as a frequency offset from f_s.

Rearranging terms and solving for C_L gives Equation 3.3. This gives the value of capacitive load as a function of the frequency offset.

$$C_L = \frac{C_m}{2\left(\frac{\Delta f_{sL}}{f_s}\right)} - C_0$$

Equation 3.3: Capacitive load expressed as a function of the frequency offset from f_s.

3.2 Temperature Compensation by Load Capacitance

It is convenient to define $\Delta f_L = f_{ext} - f_L$ as the deviation from f_L due to an external influence (i.e. a change in temperature), where f_{ext} is the altered frequency of resonance. When both a capacitive load and an ambient temperature change operate on a quartz crystal, the total frequency offset from series resonance is represented by the sum of the offsets from: f_s due to a capacitive load; and f_L due to an external influence, as shown in Equation 3.4.

$$\Delta f_s = \Delta f_{sL} + \Delta f_L$$

Equation 3.4: Total frequency offset from f_s due to the capacitive load and change in temperature.

A crystal, not subjected to a temperature change, could resonate at f_{ext} if it were presented with a capacitive load, denoted C_x. This is easily derived from Equation 3.3 by substituting Δf_s for Δf_{sL}, yielding Equation 3.5.

$$C_x = \frac{C_m}{2\left(\frac{\Delta f_s}{f_s}\right)} - C_0 = \frac{C_m}{2\left(\frac{\Delta f_{sL}}{f_s} + \frac{\Delta f_L}{f_s}\right)} - C_0$$

Equation 3.5: Capacitive load required for resonance at f_{ext}.

Going a step further, Equation 3.2 can be substituted into Equation 3.5 to express C_x in terms of the crystal's motional, static, and nominal capacitive load as in Equation 3.6. [Frerking]

$$C_x = \frac{C_m}{2\left(\frac{\Delta f_L}{f_s} + \frac{C_m}{2(C_0 + C_L)}\right)} - C_0$$

Equation 3.6: Capacitive load required for resonance at f_{ext} in terms of the crystal's motional and static capacitances, and it's nominal capacitive load.

More generally, C_x is a summation of the nominal load, C_L, plus a quantity of capacitance, ΔC_L in order to shift the parallel resonant frequency of the circuit to f_{ext}. When a crystal is subjected to a temperature change, its frequency will shift to f_{ext}. Conversely, a crystal that is not subjected to a temperature change can also resonate at f_{ext} if its parallel load capacitance shifts by ΔC_L to a new load capacitance, C_x.

In a circuit where C_L resonates with the crystal at f_L, the addition of ΔC_L to C_L will shift the parallel resonant frequency down by Δf_L when ΔC_L is positive. Inversely, when ΔC_L is a negative quantity, the frequency of resonance will increase by Δf_L.

When the temperature of the crystal changes, the resonant frequency shifts in accordance with Equation 2.11. If the magnitude of this shift is quantified as Δf_L, then the subtraction of ΔC_L from the capacitive load across the crystal can change the resonant frequency by -Δf_L and effectively compensate for the drift in frequency.

Since $C_x = C_L + \Delta C_L$, then it follows that $\Delta C_L = C_x - C_L$. For compensation of a frequency drift due to a change in temperature, $C_L - \Delta C_L$ is the necessary capacitive load, C_{L_comp}, needed in parallel with the crystal. This leads to Equation 3.7, an expression for C_{L_comp}.

$$C_{L\_comp} = 2C_L - C_x$$

Equation 3.7: Total load capacitance required for temperature compensation.

Chapter 4: Measurement of Crystal Parameters

4.1 Introduction

To design a temperature compensated crystal oscillator, the electrical equivalent circuit parameters for the crystal (Figure 2.1) and the frequency-temperature characteristic curve must be determined. There are many methods available to measure a crystal's parameters and temperature characteristics. This chapter discusses a simple, adequate procedure to evaluate them.

4.2 Equivalent Circuit Parameters

The static capacitance can easily be measured by using a capacitance meter that is sensitive enough to measure capacitance in the 1pF to 10pF range. In order to measure the motional arm parameters, the pi-networks in Figure 4.1 can be used. This network simultaneously presents the crystal with low impedances of 12.5Ω, and provides a match to standard 50Ω cables. [Salt]

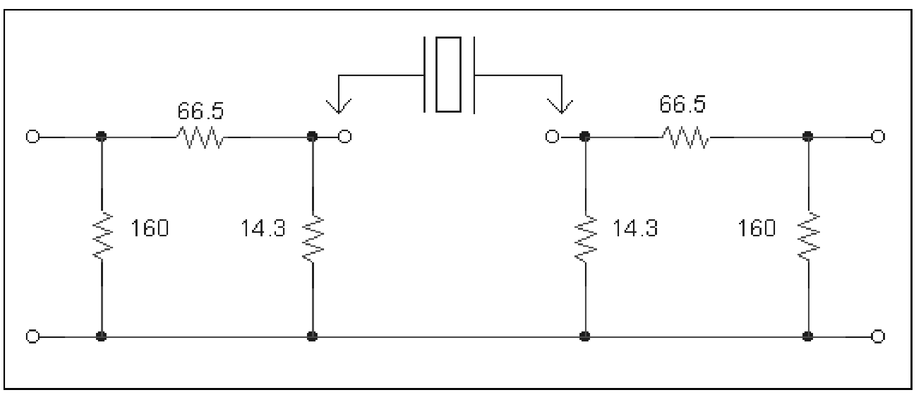

Figure 4.1: Network to measure crystal parameters.

One port of the network is driven by a signal generator, while the other is connected to the input of a spectrum analyzer. At first, the crystal is replaced by a short circuit. The power measured by the spectrum analyzer is recorded as P_{SC}. Next, the crystal is placed in the circuit and the frequency of the signal generator is adjusted until maximum power is measured. The frequency that the generator is tuned to is the series resonant frequency of the crystal. This value is recorded as f_s, and the power read off the analyzer is recorded as P_{XTL}. Then, the frequency of the signal generator is tuned in order to measure the upper and lower frequencies where the measured power is half of P_{XTL}. By subtracting the lower frequency from the upper, the 3dB bandwidth of the crystal can be calculated.

The motional arm resistance, R_m, is calculated from the ratio of the voltage measured by the spectrum analyzer with the crystal replaced by a short circuit, to that measured with the crystal in the circuit. This can be related to power (in watts) by Equation 4.1. [Salt]

$$R_m = 25\left(\sqrt{\frac{P_{SC}}{P_{XTL}}} - 1\right)$$

Equation 4.1: Calculation for the motional resistance of a crystal.

The motional capacitance is computed by Equation 4.2, where the effective resistance, R_{eff}, is equal to the sum of the crystal's motional arm resistance and the impedances presented to the crystal by the pi-networks ($R_m + 25$).

$$C_m = \frac{BW_{3dB}}{2\pi R_{eff}\, f_s^2}$$

Equation 4.2: Calculation for the motional capacitance of a crystal.

Finally, the motional arm inductance is calculated by Equation 4.3.

$$L_m = \frac{Q \cdot R_{eff}}{2\pi f_s} = \frac{f_s}{BW_{3dB}} \cdot \frac{R_{eff}}{2\pi f_s} = \frac{R_{eff}}{2\pi \cdot BW_{3dB}}$$

Equation 4.3: Calculation for the motional inductance of a crystal.

4.3 Frequency-Temperature Characteristics

The frequency-temperature characteristic curve for the crystal can be determined several different ways. The coefficients of Equation 2.11 can be determined from the physical property constants of the crystal (i.e. angle of cut, ratio of dimensions, etc.). Alternatively, the coefficients can be determined experimentally by measuring a few frequency points while the crystal is in a temperature chamber and statistically curve-fitting a cubic function to the data. Generally, the latter method is more practical because the physical property constants of the crystal are seldom available.

Chapter 5: TCXO Design

5.1 Introduction

This chapter and the next (Chapter 6) will present a practical technique to realize a crystal oscillator circuit that provides temperature compensation for an AT-cut quartz crystal. This will be achieved by working through an actual TCXO design.

5.2 Basic Oscillator Topology

A Colpitts oscillator is chosen as the topology to implement the temperature compensated crystal oscillator. This type of oscillator was chosen because it operates the crystal in the parallel resonant mode and it presents a convenient means for temperature compensation of the crystal. The basic circuit structure is shown in Figure 5.1.

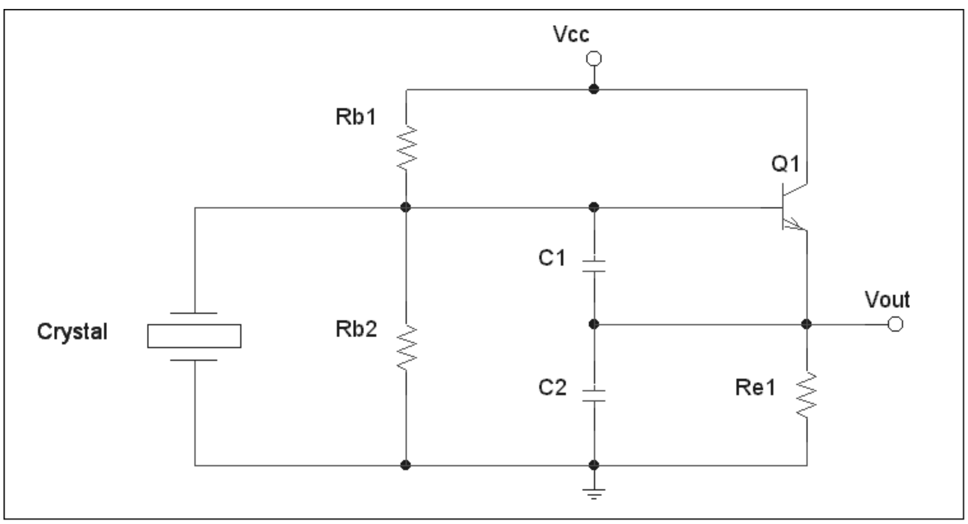

Figure 5.1: Basic structure of Colpitts Oscillator

It is often desired to follow the output of the oscillator by a grounded collector stage using a PNP transistor (see Figure 5.2). The additional stage acts as a buffer and provides isolation from the circuit it drives. It also offers the additional advantage of gaining back the voltage dropped through the base-emitter junction of the NPN transistor. For low voltage circuits (especially 5V or less), this works well to maximize output voltage swing.

The integrated structure is shown in Figure 5.2. Here, a DC blocking capacitor has been included at the oscillator's output, an AC bypass capacitor is located on the supply, and a small variable trimming capacitor has been added in series with the crystal. The capacitors C_1 and C_2 form a voltage divider and provide the feedback mechanism for oscillation to occur.

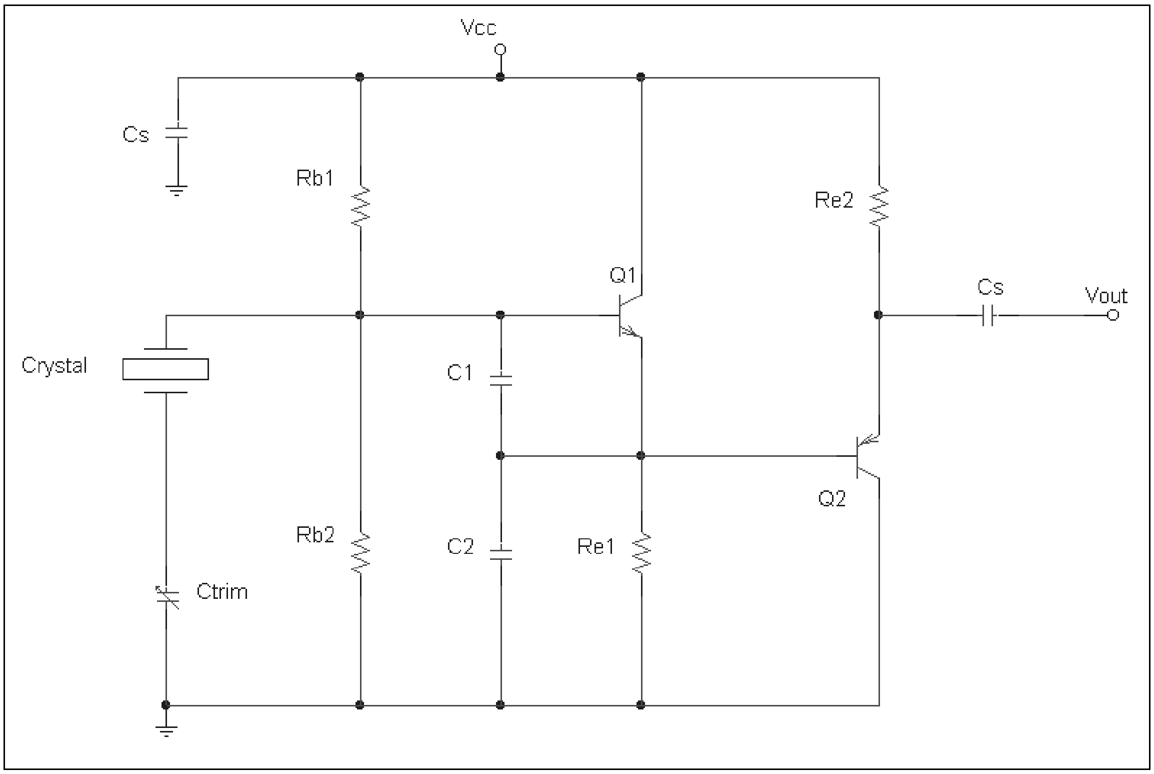

Figure 5.2: Colpitts oscillator followed by a grounded collector PNP stage.

5.3 Temperature Compensation

The effective capacitive load in parallel with the crystal is equivalent to the series combination of C_1, C_2, and C_{trim}. If C_1, C_2, and C_{trim} remain fixed over temperature (in other words they are temperature stable capacitors), then the effective capacitive load on the crystal remains constant over temperature. However, as presented in Chapter 3, in order to compensate for resonant frequency drift due to a change in temperature, the effective capacitive load, C_{L_eff}, must be temperature dependent such that its value is equal to C_{L_comp} (Equation 3.7).

Upon examination of the characteristic curves in Figure 2.3, it is apparent that in the vicinity of the nominal reference temperature, an AT-cut quartz crystal approximately exhibits a negative linear frequency-temperature relationship. This means that as the temperature decreases, the resonant frequency increases, and vice versa. To compensate for this, capacitors that have negative temperature coefficients are used for C_1 and C_2. Negative temperature coefficient (NTC) capacitors are capacitors that change value linearly (with a negative specified slope) versus temperature. They are usually characterized by a nominal capacitance at a reference temperature (usually 25°C) and a temperature coefficient in parts per million per degree Celsius (ppm/°C). The temperature coefficient is usually indicated by "Nxxx", where "N" refers to "negative slope" and "xxx" refers to the value of the coefficient. For example, a 100pF N750 capacitor will have a nominal value of 100pF at 25°C and a 750-ppm increase in capacitance for every 1-degree (Celsius) decrease in temperature. A capacitor with a zero temperature coefficient (capacitance does not change over temperature) is indicated by a "NP0" label. A capacitor's relationship for capacitance versus temperature is expressed in Equation 5.1.

$$C_{NTC} = C_{NTC\_NOM} + C_{NTC\_NOM} \times Temp\_Coeff \times 1 \cdot 10^{-6} \times (T - T_0)$$

Equation 5.1: Expression for the capacitance of a negative temperature coefficient capacitor.

If NTC capacitors are part of the crystal's parallel capacitive load, then as the temperature changes, the capacitance will change inversely. This can be used for compensation at temperatures where the characteristic curve of the crystal is approximately linear.

This strategy works well for the linear portion of the curve. However, as the temperature decreases further from the reference, the frequency vs. temperature relationship for an AT-cut crystal will reach a maximum and begin to curve back toward the nominal frequency axis (see Figure 2.3). Compensation of this bend cannot be accomplished by the NTC capacitors because they are linear functions of temperature and the frequency stability of the crystal is cubic. This non-linear behavior of the crystal requires a non-linear function of capacitance versus temperature. A way to accomplish this is to use a negative temperature coefficient thermistor in series with an NP0 (zero temperature coefficient) capacitor. An NTC thermistor is a temperature dependent resistor that has an exponential resistance-temperature relationship as shown in Equation 5.2, where R_{T_NOM} is the thermistor's nominal resistance at a reference temperature, T_0, and β is its material-specific constant.

$$R_T = R_{T\_NOM} \times e^{\beta\left(\frac{1}{T+273} - \frac{1}{T_0+273}\right)}$$

Equation 5.2: Resistance-temperature relationship for an NTC thermistor.

As the temperature of the thermistor decreases, its resistance increases exponentially. To compensate for the non-linear behavior of the crystal at low temperatures, a series circuit consisting of a thermistor and a capacitor can be used as part of the crystal's capacitive load. The thermistor should have a low resistance at room temperature so that at T_0, the parallel equivalent capacitance of the combination will be approximately equal to the value of the capacitor. As the temperature decreases, the resistance of the thermistor will increase, and as a result, the parallel equivalent capacitance of the series combination will decrease. This can compensate for the downward bend in the frequency-temperature curve.

The equivalent capacitance of the series thermistor-capacitor circuit can be determined by transforming the network into it's parallel equivalent. The series-to-parallel transformation is illustrated in Figure 5.3.

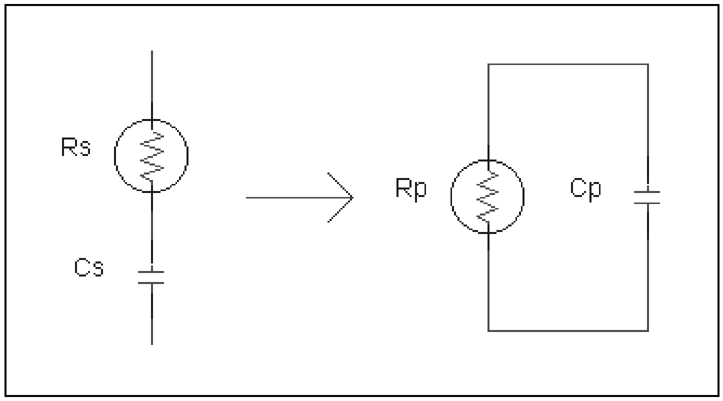

Figure 5.3: Series-to-parallel transformation.

The impedance of the series circuit is given in Equation 5.3.

$$Z_s = R_s + jX_s$$

Equation 5.3: Series impedance of the thermistor-capacitor circuit.

The equivalent parallel impedance is shown in Equation 5.4.

$$Z_p = \frac{R_p \times jX_p}{R_p + jX_p}$$

Equation 5.4: Equivalent parallel impedance of the thermistor-capacitor circuit.

The numerator and denominator of Z_p are both multiplied by the complex conjugate of its denominator. This is shown in Equation 5.5.

$$Z_p = \frac{R_p \times jX_p}{R_p + jX_p} \times \frac{R_p - jX_p}{R_p - jX_p} = \frac{R_p X_p^2 + jR_p^2 X_p}{R_p^2 + X_p^2}$$

Equation 5.5: Expression for equivalent parallel impedance of circuit.

The real and imaginary parts of Z_p are shown in Equations 5.6 and 5.7.

$$\operatorname{Re}\left[Z_p\right] = \frac{R_p X_p^2}{R_p^2 + X_p^2}$$

Equation 5.6: Real part of equivalent parallel impedance.

$$\operatorname{Im}\left[Z_p\right] = \frac{R_p^2 X_p}{R_p^2 + X_p^2}$$

Equation 5.7: Imaginary part of equivalent parallel impedance.

In order to make the transformation, the series Q and parallel Q of the circuit are set equal at the frequency of operation (Equation 5.8).

$$Q = Q_s = Q_p = \frac{|X_s|}{R_s} = \frac{R_p}{|X_p|}$$

Equation 5.8: Expression equating Q_s to Q_p.

Making the substitution for Q into the real and imaginary parts of Z_p yields Equations 5.9 and 5.10.

$$\operatorname{Re}\left[Z_p\right] = \frac{1}{Q^2 + 1} R_p$$

Equation 5.9: Real part of Z_p with substitution of Q.

$$\operatorname{Im}\left[Z_p\right] = \frac{Q^2}{1 + Q^2} X_p$$

Equation 5.10: Imaginary part of Z_P with substitution of Q.

In order for Z_s to equal Z_p, both the real parts and the imaginary parts must be equal. Equating the real and imaginary parts gives the relationships between R_p and R_s and between X_p and X_s that are presented in Equations 5.11 and 5.12.

$$R_s = \frac{1}{1+Q^2} R_p \Rightarrow R_p = \left(1+Q^2\right) R_s = \left(1 + \left(\frac{X_s}{R_s}\right)^2\right) R_s$$

Equation 5.11: Relationship between the series resistance and parallel equivalent resistance of the thermistor-capacitor circuit.

$$X_s = \frac{Q^2}{1+Q^2} X_p \Rightarrow X_p = \frac{1+Q^2}{Q^2} X_s = \frac{1+\left(\frac{X_s}{R_s}\right)^2}{\left(\frac{X_s}{R_s}\right)^2} X_s$$

Equation 5.12: Relationship between the series reactance and parallel equivalent reactance of the thermistor-capacitor circuit.

To simplify the relationship between X_p and X_s (in Equation 5.12), the numerator and denominator of X_P are divided by $\left(\frac{X_s}{R_s}\right)^2$. This results in Equation 5.13.

$$X_p = X_s \left[\left(\frac{R_s}{X_s}\right)^2 + 1\right]$$

Equation 5.13: Simplified relationship between X_p and X_s

Since $X_p = \frac{1}{\omega C_p}$ and $X_s = \frac{1}{\omega C_s}$, the equivalent parallel capacitance of the series thermistor-capacitor circuit can be expressed in terms of the series capacitor value, the value of resistance of the thermistor and the frequency of operation (Equation 5.14).

$$\frac{1}{\omega C_p} = \frac{1}{\omega C_s}\left(R_s^2 \omega^2 C_s^2 + 1\right) \Rightarrow C_p = \frac{C_s}{1 + \omega^2 R_s^2 C_s^2}$$

Equation 5.14: Expression for equivalent parallel capacitance of thermistor-capacitor network.

From Equation 5.14, it is easily seen that as the resistance of the thermistor increases exponentially (when the temperature decreases) the effective parallel capacitance of the network decreases exponentially.

The same idea can be used for compensation at high temperatures where the frequency-temperature curve deviates from its linearly decreasing trend and begins to increase (see Figure 2.3). The major difference would be to use a thermistor that has a large value of resistance at room temperature so that its equivalent parallel capacitance at that temperature is very small. As the temperature increases, the thermistor resistance will decrease exponentially, and cause the equivalent parallel capacitance to increase. The best placement for this series thermistor-capacitor circuit is directly in parallel with the crystal so that its capacitance is in parallel with the rest of the load. Since values of capacitance add when in parallel, an increase or decrease in the equivalent capacitance of the thermistor-capacitor circuit will cause a direct increase or decrease in the crystal's total capacitive load.

Figure 5.4 shows the addition of the negative temperature coefficient capacitors and the thermistor-capacitor circuits into the base oscillator circuit of Figure 5.2. The compensation at low temperatures is accomplished by RT_1 and C_{cold}, while RT_2 and C_{hot} provide compensation at high temperatures. This is a complete schematic for the temperature compensated crystal oscillator (TCXO).

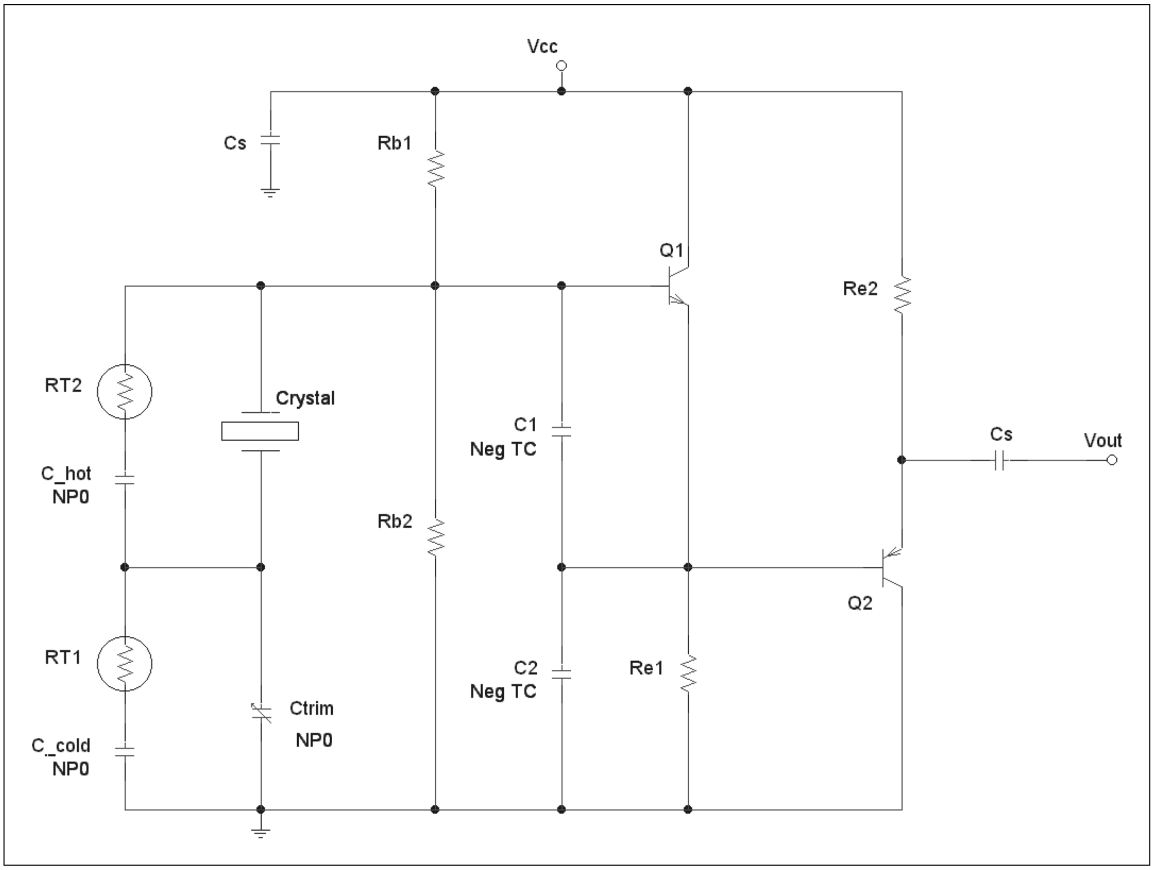

Figure 5.4: Complete TCXO circuit.

An expression for the total capacitive load presented across the crystal's terminals can be determined. The value of C_{cold_Equiv} (the equivalent parallel capacitance of RT_1 and C_{cold}) and C_{trim} are in parallel. This parallel combination is in series with C_1 and C_2. This total series combination is in parallel with C_{hot_Equiv} (the equivalent parallel capacitance of the thermistor-capacitor circuit, RT_2 and C_{hot}). The complete expression is shown in Equation 5.15.

$$C_{Total} = \left[\frac{1}{C_{trim} + C_{cold\_Equiv}} + \frac{1}{C_1} + \frac{1}{C_2} \right]^{-1} + C_{hot\_Equiv}$$

Equation 5.15: Total capacitive load presented across the crystal.

5.4 Selecting Component Values

The values of the capacitors and thermistors can be determined conveniently using a math software package. The program listed in Appendix A is a MATLAB script file that was created to help design a temperature-compensation network based on the topology shown in Figure 5.4. A user's guide to the script can be found in Appendix B.

The designer inputs the equivalent circuit parameters of the crystal and its frequency-temperature data. The program calculates C_{L_comp} (using the theory presented in Chapter 3), and plots the result versus temperature. Next, by the process outlined in Appendix B, the designer chooses values for the thermistors and capacitors. Equations 5.1, 5.2, 5.14, and 5.15 are used to calculate the values of capacitance for C_1 and C_2, the resistance of the thermistors, the equivalent parallel capacitance of the thermistor-capacitor circuits, and the total capacitive load over the specified temperature range, respectively. The value of the trimmer capacitor, C_{trim}, required to tune the resonant frequency of the oscillator to the desired frequency at the reference temperature is also calculated. This value of trimmer capacitance is computed by solving Equation 5.15 for C_{trim}, and then substituting the nominal values for the thermistors, capacitors, and total load capacitance at room temperature into the resulting equation (Equation 5.16).

$$C_{trim} = \left[\frac{1}{C_{L\_Nom} - C_{hot\_Equiv\_Nom}} - \frac{1}{C_{1\_Nom}} - \frac{1}{C_{2\_Nom}} \right]^{-1} - C_{cold\_Equiv\_Nom}$$

Equation 5.16: Expression to calculate value of trimmer capacitor.

After the trimmer capacitor value is calculated, the total temperature-dependent capacitive load, C_{Total}, is computed, using Equation 5.15, over the temperature range of interest. This result is plotted on the same graph as C_{L_comp} (see Figure 6.6). This allows the designer to get a visual understanding of the behavior of the circuit, and to analyze its performance graphically. The chosen component values can be modified in order to minimize the error between C_{L_comp} and C_{Total}.

The frequency error, as a function of temperature, can be predicted for the circuit values selected by calculating the difference between the total capacitance of the circuit and the required capacitive load (C_{Total} - C_{L_comp}). By adding this error, C_{Error}, to the nominal value of capacitive load (C_{L_Nom}), Equation 3.2 can be used to determine the total frequency offset, Δf, from series resonant frequency, f_s as a function of C_{Error}. This is shown in Equation 5.17.

$$\Delta f = f_s \times \frac{C_m}{2\left(C_0 + C_{L\_Nom} + C_{Error}\right)}$$

Equation 5.17: Frequency offset from f_s as a function of C_{Error}

From Equation 5.17, the error in frequency from the desired operating frequency, f_L, can be calculated by adding Δf to f_s and then subtracting f_L as in Equation 5.18.

$$f_{Error} = \left(\Delta f + f_s\right) - f_L$$

Equation 5.18: Calculation for frequency error

A graph of the predicted frequency error (plotted in units of parts per million) will provide a good estimation of whether the design meets the requirements. This graph can also be used an easy tool to determine the exact nominal load capacitance that the crystal needs for resonance at the desired frequency (given the measured crystal parameters). This can be accomplished by setting C_{Error} equal to zero and adjusting the value of C_{L_Nom} until f_{Error} equals zero.

Chapter 6: TCXO Implementation and Verification

6.1 Introduction

This chapter will continue the design of a temperature-compensated crystal oscillator using the circuit topology and temperature compensation techniques that were presented in Chapter 5. The user's guide in Appendix B will be used in conjunction with the MATLAB script in Appendix A to determine component values and verify the performance of the design.

6.2 TCXO Requirements

The oscillator is required to resonate at 12.8 MHz with a frequency stability of ≤ 2.5ppm over a temperature range from -20°C to +55°C. The circuit is required to operate from a 3.3V supply.

6.3 Circuit Design

The transistor is biased such that the dc emitter current, I_E, is approximately 500μA, and V_{CE} is 2.3V. The resulting bias circuit is illustrated in Figure 6.1.

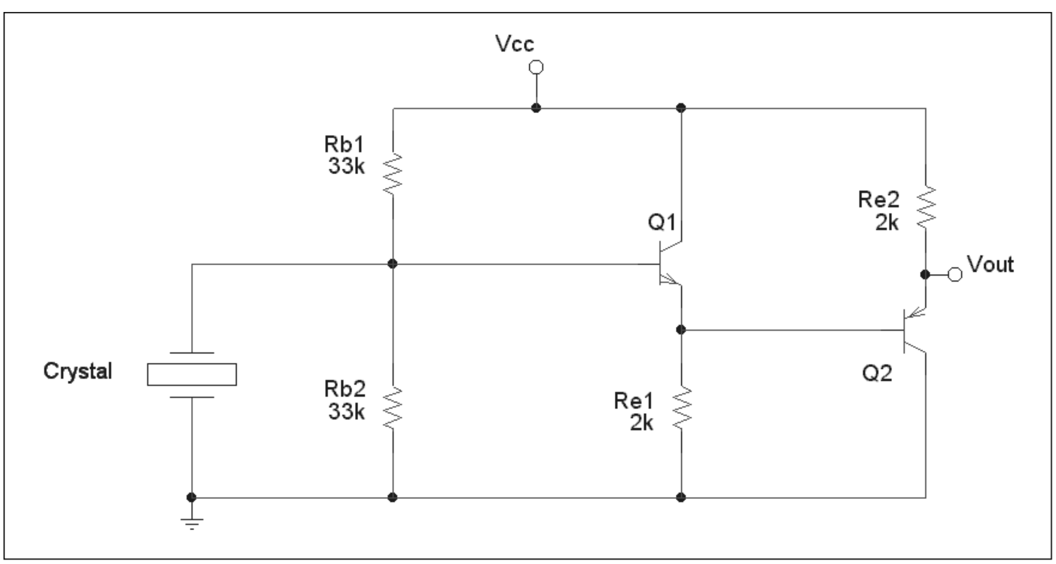

Figure 6.1: DC bias of the oscillator.

The crystal chosen for the design is an AT-cut quartz unit that was fabricated for parallel resonance at 12.8MHz when presented with approximately a 32pF load capacitance. The crystal is housed in a 7.5mm x 5.2mm surface mount package. Some parameters for the equivalent circuit model (motional arm and static capacitance) as well as series resonant frequency were supplied by the vendor. If they were not, the procedures outlined in Chapter 4 would have been followed to determine the values. The parameters are listed in Table 6.1.

Table 6.1: Equivalent circuit model parameters for an AT-cut quartz crystal.

Parameter	Value
C_m	6.1×10^{-15} F
C_0	2.0×10^{-12} F
f_s	12.798913×10^{6} Hz

A small temperature chamber was constructed for the project. The frequency-temperature characteristic curve of the crystal is determined by implementing the Colpitts oscillator with NP0 capacitors to present a temperature-stable load of approximately 32pF for resonance at 12.8MHz. The circuit is shown in Figure 6.2.

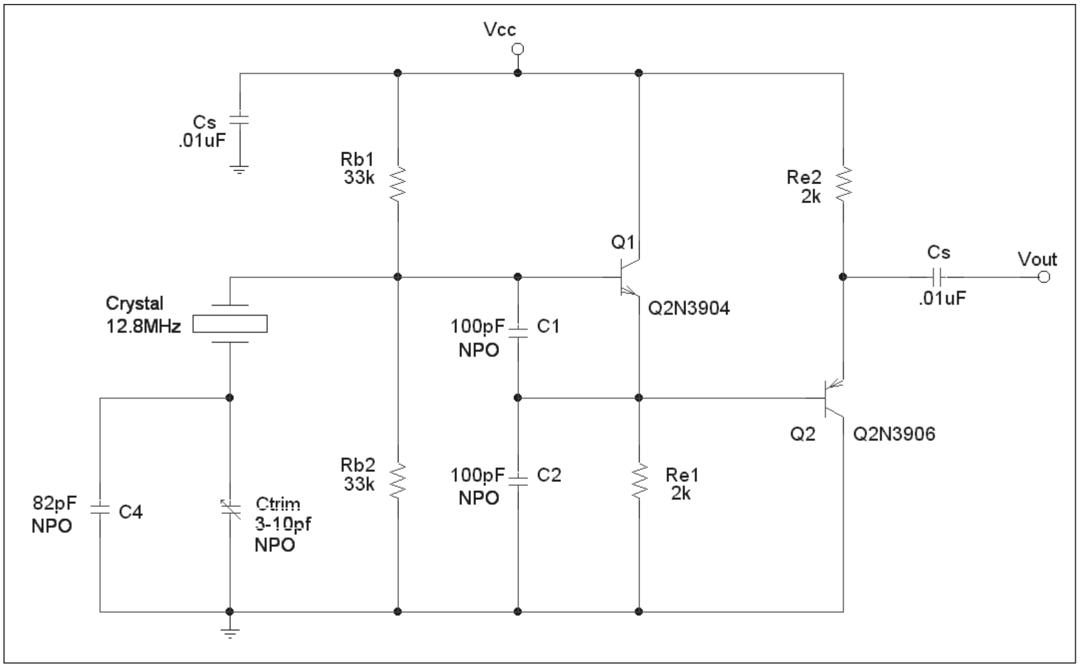

Figure 6.2: Circuit used to measure frequency-temperature characteristic curve of crystal

The trimmer is adjusted until the resonant frequency measures as close as possible to 12.8MHz at room temperature. The circuit is then placed inside the temperature chamber. As the temperature is varied from approximately -20°C to +70°C, frequency measurements are taken at various temperatures and recorded in Table 6.2.

Table 6.2: Measured frequency-temperature data for crystal

Temperature (°C)	Frequency (MHz)
-22.9	12.799931
-10.3	12.800002
-0.8	12.800023
15.4	12.800018
25.0	12.799999
35.0	12.799982
52.2	12.799960
69.8	12.799990

This measurements are entered into the MATLAB script (Appendix A) and a cubic function is fit to the data. The resulting cubic curve is graphed in Figure 6.3.

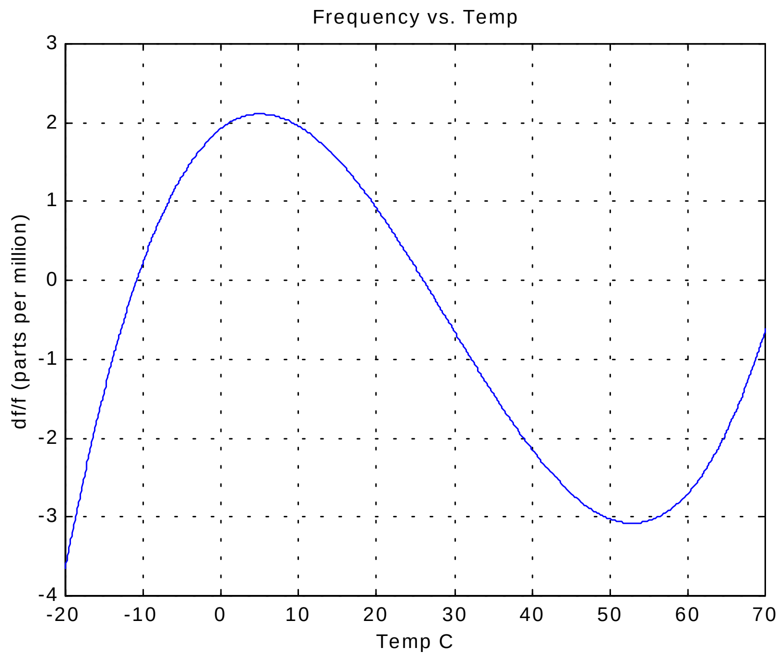

Figure 6.3: Cubic approximation for frequency-temperature data of crystal

The equivalent circuit parameters and series resonant frequency of the crystal are entered into the script and the exact nominal capacitive load is determined for a resonant frequency of 12.8MHz. This value turned out to be 33.91pF.

With this information about the crystal, the required capacitive load for compensation, C_{L_Comp}, is computed and plotted versus frequency in Figure 6.4.

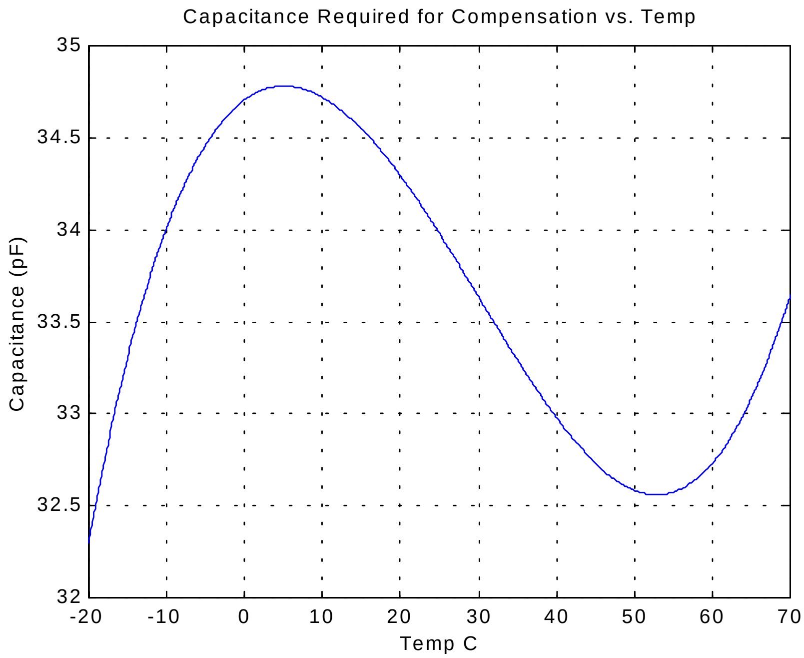

Figure 6.4: Graph of capacitive load required for compensation, C_{L_Comp}, vs. temperature

The theory that was presented in Chapter 5, including Figure 5.4 as a template for the circuit design, was used to design the TCXO.

The design of the circuit is a trial and error process. The component values are initially chosen and entered into the MATLAB script (Appendix A) for simulation. The results are analyzed and the component values are modified in an iterative process until the predicted frequency error is within the design limits.

First, values for the negative temperature coefficient capacitors C_1 and C_2 are selected to approximate the negative-slope linear portion of C_{L_comp}. Next, the thermistor-capacitor sub-circuits are designed to compensate for the changes in concavity at low temperatures and at high temperatures. Figure 6.5 shows the final values for the design.

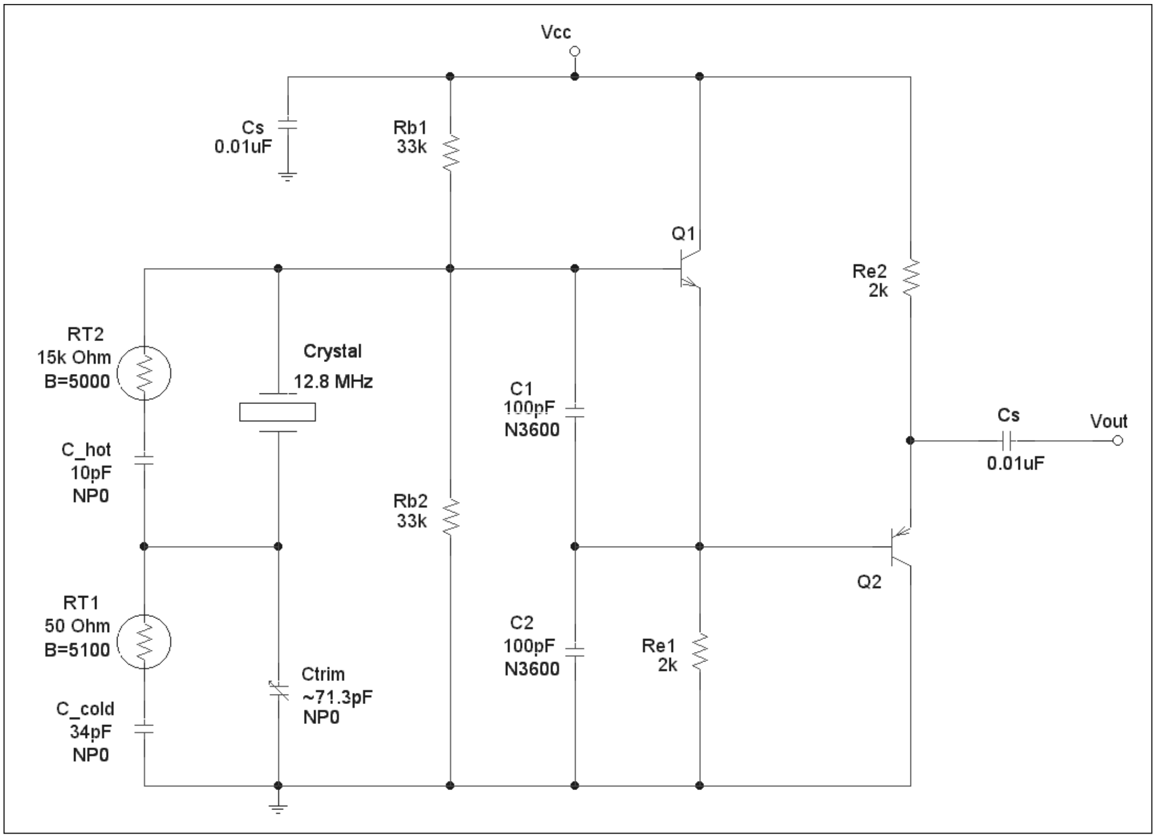

Figure 6.5: Schematic of TCXO

Figure 6.6 shows C_{Total} for the circuit and C_{L_comp} graphed versus temperature. Ideally, for perfect temperature compensation, the two curves would be identical. Since they are not, there will be some predicted error in frequency. The error is calculated and shown in Figure 6.7.

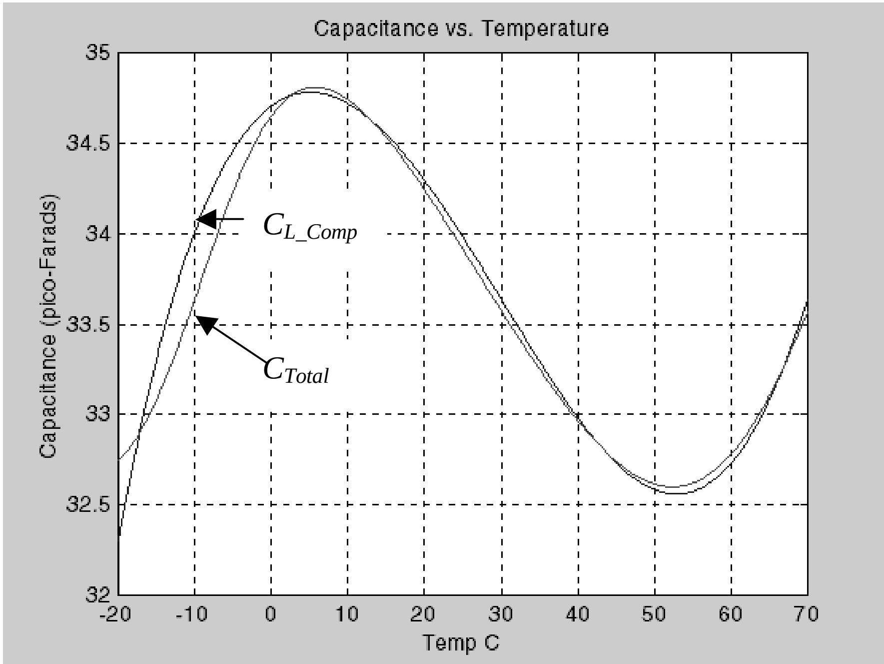

Figure 6.6: Comparison of total capacitance of the circuit (C_{Total}) with required capacitance for compensation (C_{L_Comp}).

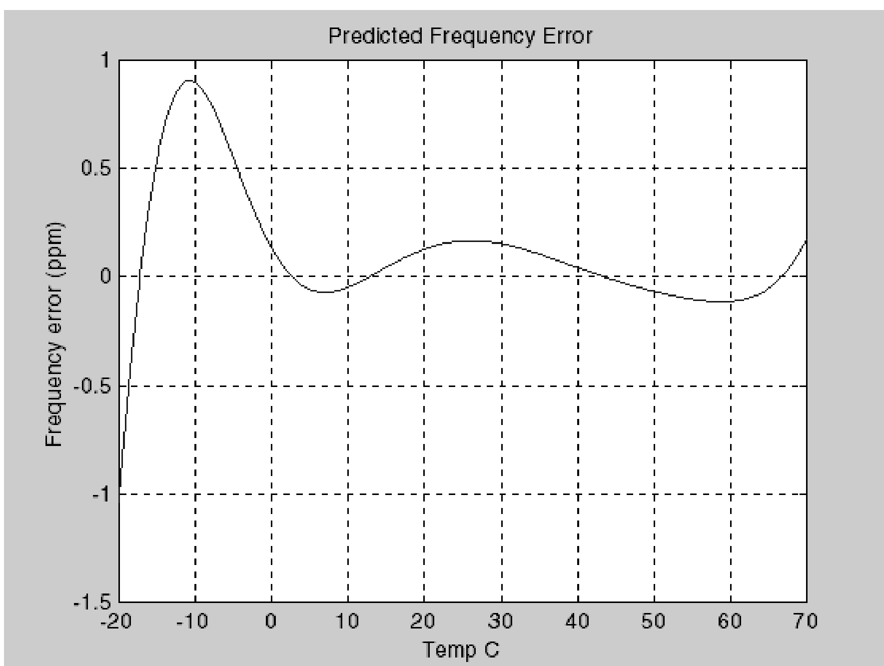

Figure 6.7: Predicted frequency error of TCXO circuit

The initial temperature compensation goal was to improve the frequency stability of the crystal to within ±2.5ppm over the temperature range of -20°C to +70°C. However, given the limited values of NTC capacitors and thermistors available to use at the time of implementation, the project became an exercise to prove the validity of the theory and design process. Only one of the thermistor-capacitor sub-circuits is realized, just for the low-temperature compensation. The largest temperature coefficient on hand for C_1 and C_2, in the 100pF range, was N750. Using the N750 capacitors, the thermistor and NP0 capacitor were chosen so the low temperature frequency error of the crystal (Figure 6.3) could be improved while at least maintaining or slightly improving the error over the rest of the temperature range. Figure 6.8 shows the values for the TCXO that was actually implemented.

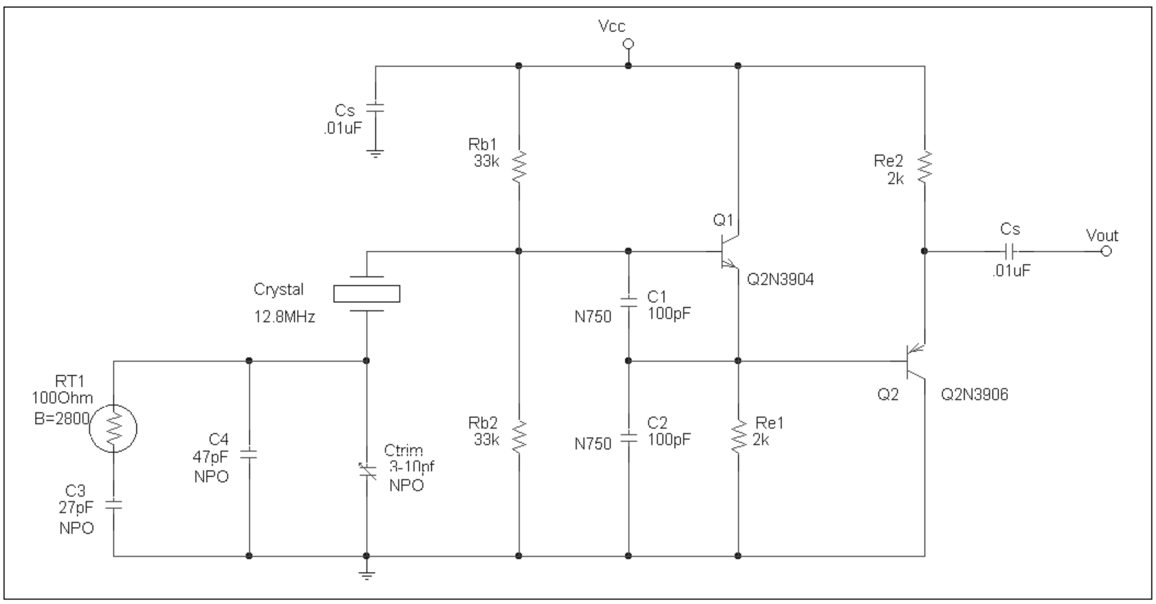

Figure 6.8: Schematic of the TCXO that was implemented.

Figure 6.9 shows the crystal's total temperature-dependant capacitive load, C_{Total}, plotted on the same graph as the required capacitive load, C_{L_Comp}, versus temperature. From this graph, it is obvious that the values chosen are not optimal – only the best solution given the limited resources. It is again stated that the purpose of this exercise was to demonstrate and validate the proposed technique for temperature compensation.

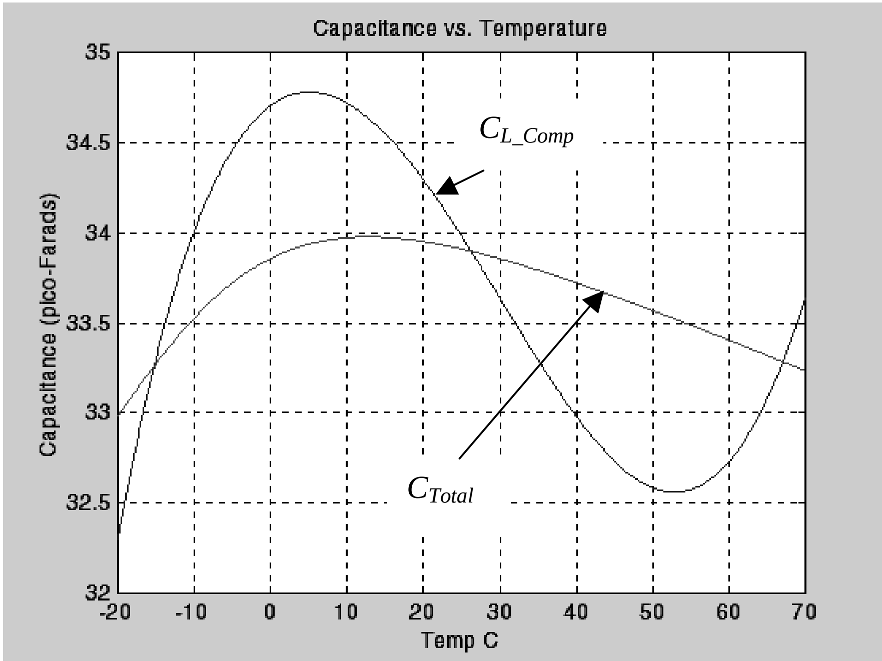

Figure 6.9: Comparison of total capacitance (C_{Total}) with required capacitance (C_{L_Comp}) for the TCXO circuit that was implemented.

The predicted frequency error for the circuit is given in Figure 6.10.

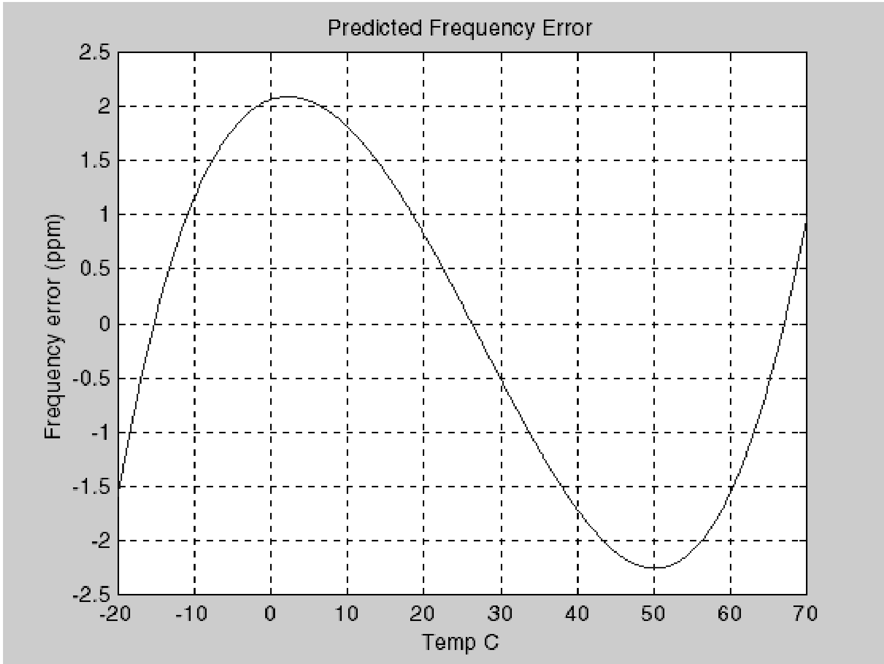

Figure 6.10: Predicted frequency error of TCXO circuit that was implemented

6.4 Implementation of TCXO

The TCXO (Figure 6.8) was constructed with the values shown and the frequency of the oscillator was measured over temperature (approximately from -20°C to +70°C). The data from the experiment is listed in Table 6.3 and graphed in Figure 6.11.

Table 6.3: Measured results from TCXO circuit

Temperature (°C)	Frequency (MHz)
-22.6	12.799991
-10.2	12.800022
-0.6	12.800028
15.3	12.800019
25.1	12.800003
34.6	12.799986
50.5	12.799971
69.9	12.800010

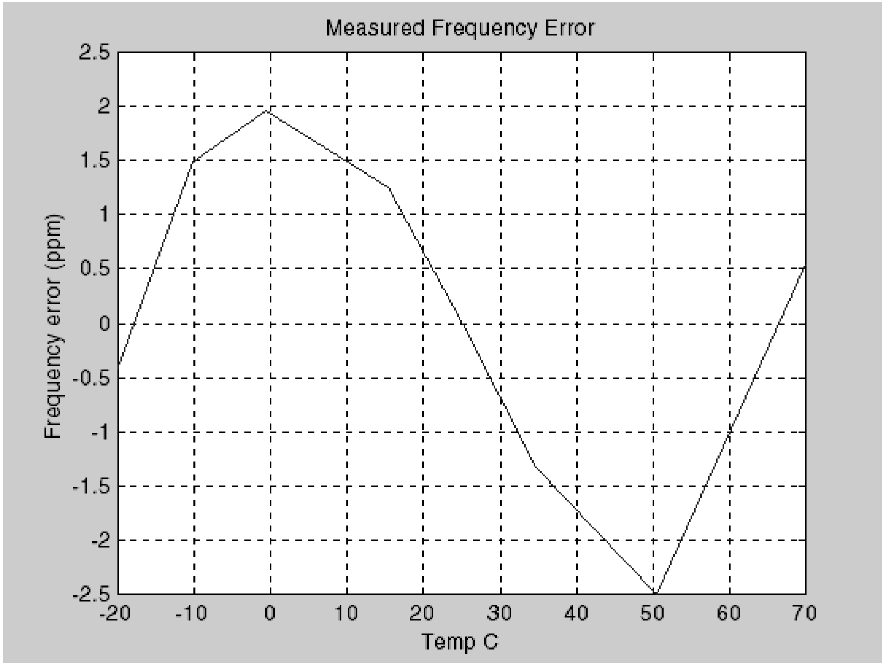

Figure 6.11: Experimental results of the TCXO frequency error over temperature

The measured error in Figure 6.11 is close to the predicted frequency error in Figure 6.10. Although the results do not show much improvement in frequency stability over the crystal without temperature-compensation (Figure 6.3), it does demonstrate that the theory developed in this paper is fundamentally correct.

Conclusion

This paper presented the theory of temperature compensation and a procedure for implementing that theory and predicting its performance. Specifically, a design for a temperature-compensated crystal oscillator (TCXO) was presented. The AT-cut crystal was the center of the theory and design. From its electrical equivalent circuit model, equations for series and parallel resonant frequencies were derived. AT-cut crystals exhibit frequency stability characteristics that can be accurately approximated by cubic mathematical functions. The function's coefficients for a particular crystal can be determined easily by measurement, or by knowledge of the crystal's extensive physical properties. By designing the circuit such that the crystal will be operated in parallel resonance with an external capacitance, equations were derived that express the frequency stability of the crystal oscillator as a function of the crystal's capacitive load. This relationship led to the development of the theory of temperature compensation by a crystal's external load capacitance.

The first step of the design process is to characterize the crystal. The electrical equivalent circuit parameters of the crystal, as described in Chapter 2, are required as well as its frequency-temperature characteristic curve. These parameters are sometimes provided by the crystal manufacturer or can be easily determined by measurement (Chapter 4). After information about the crystal is obtained, the equations developed in Chapter 3 are used to calculate the capacitive load required for compensation, C_{L_Comp}. Next in Chapter 5, a circuit topology was developed and an equation for the total capacitive load presented across the crystal, C_{Total} (Equation 5.11), was derived. Using the design equations for C_{L_Comp} and C_{Total}, values for the capacitors and thermistors can be determined, by an iterative process, to provide the required frequency stability. The MATLAB script listed in Appendix A is a convenient tool to determine the component values, as well as to calculate the predicted frequency error of the oscillator.

An example of the TCXO design process was described in Chapter 6. A circuit was designed and simulated in MATLAB, yielding good temperature stability. However, resources were limited and a less desirable circuit was constructed in the lab. This design did not demonstrate the performance that could have been achieved, but it did show that the measured results could be accurately predicted by the theory presented in this paper.

This project encountered a number of problems. Foremost, negative temperature coefficient capacitors were available in only a limited selection of temperature coefficients. This constraint meant that the TCXO circuit would only compensate crystals with limited degrees of frequency stability, leading to tighter requirements for the crystal. It was difficult to obtain crystals that satisfied the specification for stability while also meeting strict physical size requirements.

Further work on this subject might include research into different oscillator architectures that could possibly lend themselves to more flexible temperature compensation techniques. Some different topologies might help to overcome the design and performance restrictions imposed by the limited availability of negative temperature coefficient capacitors.

Appendix A: MATLAB Script

```
% TCXO_design_aid.m
% Script to aid design of TCXO

clear all; close all; clc;

%%%%%%%%%%%%%%%%%%%%%%%%%%%%%%%%%%%%%%%%%%%%%%%%%%%%%%%%%%%%%%%%%%%%%%%%%%
% Section 1: Enter Crystal Parameters

Cm=6.1e-15;             %motional capacitance
C0=2.0e-12;             %parallel capacitance
f_series=12.798913e6;   %measured series resonant frequency
                        %of the crystal

CL_nom=33.91e-12;    %load capacitance for resonance at f0
                     %(this value should be adjusted so that f_error
                     %is minimized when del_CL=0)

T0=25;               %nominal temp (for normalization)

f_nom=12.799999e6;   %frequency at T0 for crystal's freq_Temp data

w=2*pi*12.8e6;

T=-20:0.1:70;        %temp range


%%%%%%%%%%%%%%%%%%%%%%%%%%%%%%%%%%%%%%%%%%%%%%%%%%%%%%%%%%%%%%%%%%%%%%%%%%
% Section 2: Plot Frequency vs. Temperature
%
% Draw freq vs. temp curve for AT cut crystal.

% Method 1: Use AT coefficients given by Gerber & Ballato [p101]:
% ref: (Gerber & Ballato, "Precision Frequency Control, Vol. 2", 1985)
% Angle determines frequency tolerance.

Theta_0 = 35.25;        %ref angle that produces a zero TC slope at
                        %the ref temp
del_Theta = 1.7/60;     %# of minutes off ref angle to produce desired
                        %curve

A1 = -5.08e-6 * del_Theta;
A2 = -0.45e-9;
A3 = 108.6e-12;

curve1 = A1*(T-T0)+A2*(T-T0).^2+A3*(T-T0).^3;

%%%%%%%%%%

% Method 2: Measure crystal.
% Data for freq vs. temp curve of crystal (taken experimentally)
temp=[-22.9 -10.3 -0.8 15.4 25.0 35.0 52.2 69.8];
```

```
freq=[12.799931e6 12.800002e6 12.800023e6 12.800018e6 12.799999e6
12.799982e6 12.799960e6 12.799990e6];

del_f2=freq - f_nom;
f_rel=del_f2 / f_series;

% Fit cubic function to data
coeffs=polyfit(temp,f_rel,3);

% Generate curve
curve2=coeffs(4) + coeffs(3).*T + coeffs(2).*T.^2 + coeffs(1).*T.^3;

%%%%%%%%%%

% Plot freq vs. temp curves
figure(1);
plot(T,curve2*1e6);        %Change to "curve1" if Method 1 is used.
grid on;
title('Frequency vs. Temp');
xlabel('Temp C');
ylabel('df/f (parts per million)');


%%%%%%%%%%%%%%%%%%%%%%%%%%%%%%%%%%%%%%%%%%%%%%%%%%%%%%%%%%%%%%%%%%%%%%%
% Section 3: Determine Capacitive Load for Temperature Compensation


Cx=Cm./(2.*(curve2+Cm./(2*(C0+CL_nom))))-C0;   % Frerking (eq. 10-6)
      % ref: (Frerking, "Crystal Oscillator Design & Temperature
      % Compensation", 1978)


CL_comp=2*CL_nom-Cx;

% This is the required capacitive load needed for compensation.

figure(2);
plot(T,CL_comp*1e12);
grid;
title('Capacitance Required for Compensation vs. Temp');
xlabel('Temp C');
ylabel('Capacitance (pF)');


%%%%%%%%%%%%%%%%%%%%%%%%%%%%%%%%%%%%%%%%%%%%%%%%%%%%%%%%%%%%%%%%%%%%%%
% Section 4: Determining Temperature-Compensating Parameters
%
% Now simulate effective capacitance of circuit across crystal and
% overlay results on predicted compensating capacitance curve

% TCXO component values (adjustable parameters):

C_cold=27e-12;          %value of fixed NPO cap (cold end)
C_hot=00e-12;           %value of fixed NPO cap (hot end)
RT1_BETA=2800;          %beta of thermistor 1 (cold end) (B25/50)
RT1_nom=100;           %zero-power resistance of thermistor 1 at 25C
RT2_BETA=5000;          %beta of thermistor 2 (hot end) (B25/85)
```

```
RT2_nom=15e3;           %zero-power resistance of thermistor 2 at 25C
Cntc1_nom=100e-12;      %nominal capacitance of Cntc1 at 25C
Cntc1_temp_coeff=0750;  %Neg temp coeff of Cntc1 in ppm
Cntc2_nom=100e-12;      %nominal capacitance of Cntc2 at 25C
Cntc2_temp_coeff=0750;  %Neg temp coeff of Cntc2 in ppm

% Calculate value of Neg TC caps and thermistors as functions of temp

Cntc1_slope = Cntc1_nom*Cntc1_temp_coeff*1e-6;
Cntc1 = Cntc1_nom - Cntc1_slope.*(T-T0);
Cntc2_slope = Cntc2_nom*Cntc2_temp_coeff*1e-6;
Cntc2 = Cntc2_nom - Cntc2_slope.*(T-T0);
RT1=RT1_nom.*exp(RT1_BETA*(1./(T+273)-1/(T0+273)));
RT2=RT2_nom.*exp(RT2_BETA*(1./(T+273)-1/(T0+273)));


% Calculate equivalent capacitance of thermistor-capacitor legs that
% the xtal will see

% (Equivalent parallel capacitance - cold end)
C_cold_equiv=C_cold./(1+(w^2*C_cold^2*RT1.^2));

% (Equivalent parallel capacitance at 25C)
C_cold_equiv_nom=C_cold./(1+(w^2*C_cold^2*RT1_nom.^2));

% (Equivalent parallel capacitance - hot end)
C_hot_equiv=C_hot./(1+(w^2*C_hot^2*RT2.^2));

% (Equivalent parallel capacitance at 25C)
C_hot_equiv_nom=C_hot./(1+(w^2*C_hot^2*RT2_nom.^2));

% Calculate fixed capacitor value and total effective capacitance
% across crystal.
Cfixed=1./(1/(CL_nom-C_hot_equiv_nom)-1/Cntc1_nom-1/Cntc2_nom)-
C_cold_equiv_nom

Ctotal=1./(1./(Cfixed+C_cold_equiv)+1./Cntc1+1./Cntc2)+C_hot_equiv;


% Plot both required capacitance and actual equivalent capacitance from
% component values specified.
figure(3);
plot(T,CL_comp*1e12, T,Ctotal*1e12);
grid;
title('Capacitance vs. Temperature');
xlabel('Temp C');
ylabel('Capacitance (pico-Farads)');


%%%%%%%%%%%%%%%%%%%%%%%%%%%%%%%%%%%%%%%%%%%%%%%%%%%%%%%%%%%%%%%%%%%%%%%
% Section 5: Calculate Predicted Frequency Error

%C_error = 0;        %this is for CL_nom calibration

% Calculate difference between curves:
C_error = Ctotal-CL_comp;
```

```
% Calculate difference from series resonant frequency:
del_f = f_series*Cm./(2*(C0+CL_nom+C_error));

% Calculate difference from nominal frequency (freq at CL load):
f_error = (del_f + f_series) - 12.8e6;

% Normalize to nominal freq:
f_error_ppm = f_error / 12.8e6 * 1e6;

% Plot predicted frequency error
figure (4);
plot(T,f_error_ppm);
grid;
title('Predicted Frequency Error');
xlabel('Temp C');
ylabel('Frequency error (ppm)');


%%%%%%%%%%%%%%%%%%%%%%%%%%%%%%%%%%%%%%%%%%%%%%%%%%%%%%%%%%%%%%%%%%%%%%
% Section 6: Plot Measured Results of TCXO Circuit

% Measured data:
temp0=[-22.6 -10.2 -0.6 15.3 25.1 34.6 50.5 69.9];
freq0=[12.799991e6 12.800022e6 12.800028e6 12.800019e6 12.800003e6
12.799986e6 12.799971e6 12.800010e6];
f0=12.800003e6;
del_f0=freq0 - f0;
f_rel_0=del_f0 / f0;   %normalize to frequency at 25C


% Plot result
figure (5);
plot (temp0,f_rel_0*1e6)
grid on;
title('Measured Frequency Error');
xlabel('Temp C');
ylabel('Frequency error (ppm)');
axis([-20 70 -2.5 2.5]);
```

Appendix B: User's Guide to MATLAB Script

The MATLAB script in Appendix A was written to aid in the design of a TCXO based on the circuit topology shown in Figure 5.4. This user's guide is intended to provide a systematic approach to choosing component values and verifying the performance of a design. The script can be copied directly from Appendix A to a MATLAB Editor/Debugger window and saved as a "*.m" file.

Step 1: Determine Crystal Parameters

Determine the crystal's electrical equivalent circuit parameters (see Figure 2.1). These are sometimes provided by the manufacturer of the crystal. If not, the procedures described in Chapter 4 can be used to measure them. Once the parameters are determined, they can be entered into Section 1 of the MATLAB script. Also entered are the reference temperature, T_0, the nominal operating frequency, f_{nom}, and the temperature range, T.

Step 2: Determine Nominal Load Capacitance

The next step is to determine the exact value of C_{L_Nom} for resonance at the desired nominal frequency, f_{nom}. One way to do this is to set C_{Error} equal to zero (comment out actual line for C_{Error}) and then simulate the predicted frequency error. A plot of "Predicted Frequency Error" will be generated as the script executes. Adjust C_{L_Nom} and re-execute the script until the predicted frequency error is nearly zero. When the value is determined, set C_{Error} back to its original equation.

Step 3: Determine Frequency-Temperature Curve

Determine the frequency-temperature characteristic curve for the crystal. The coefficients given by Gerber and Ballato can be used if physical properties of the crystal are known. Otherwise, frequency data can be measured over temperature as explained in Chapter 4. The data points can be entered into Section 2 of the script.

Step 4: Determine Values for NTC Capacitors

Values for the negative temperature-coefficient capacitors should be determined first. Enter initial values for nominal capacitance and temperature coefficients into Section 4, and then execute the script. Adjust the values until the capacitance of the circuit closely approximates the negative-sloped segment of the required load capacitance, C_{L_comp}. This is shown in the plot of "Capacitance vs. Temperature" that is generated by the script.

Step 5: Determine Values for Thermistor-Capacitor Circuits

After the NTC capacitor values have been determined, the cold-end and high-end thermistor-capacitor values can be determined. Start with an initial capacitor value and a nominal resistance and beta for one of the thermistor-capacitor circuits. Enter the values into Section 4 of the script and run it. Adjust the values until the capacitance of the circuit is as close as possible to the required load capacitance. Check the plot of "Predicted Frequency Error" for acceptable results. Next, do the same for the remaining thermistor-capacitor circuit. There will be some interaction with the first circuit and the NTC capacitors, so some fine-tuning of the entire circuit may be required.

Step 6: Measure the TCXO

Finally, measure the performance of the TCXO over temperature. Frequency-temperature data points can be entered into Section 6 of the MATLAB script. The results will be plotted in the figure titled "Measured Frequency Error".

References

Frerking, Marvin E. *Crystal Oscillator Design and Temperature Compensation*, New York: Van Nostrand, 1978.

Gerber, Eduard A., and Arthur Ballato. *Precision Frequency Control, Volume 2 "Oscillators and Standards"*, Orlando: Academic Press, 1985.

Salt, David. *Hy-Q Handbook of Quartz Crystal Devices*, Wokingham: Van Nostrand Reinhold, 1987.

Bechmann, Rudolf. "Frequency-Temperature-Angle Characteristics of AT-Type Resonators Made of Natural and Synthetic Quartz," *Proceedings of the IRE*, November 1956, pp. 1600-1607.

Ueno, Yoshifusa. "Temperature-Compensated Crystal Oscillators," *Electronics and Communications in Japan*, Part 2, Vol. 79, No. 2, 1996, pp. 9-23.

Hewlett-Packard. "Application Note 200-2: Fundamentals of Quartz Oscillators," 1997.

VITA

Mark Haney was born on February 21, 1975 in Lakewood, California. He lived in California until graduating from Mission San Jose High School, in Fremont, in June 1993. He then moved to Prescott, Arizona to pursue his undergraduate studies at Embry-Riddle Aeronautical University. Mark graduated with honors and received his Bachelor of Science degree in Electrical Engineering in December of 1997.

After graduation, Mark moved to Blacksburg, Virginia to attend Virginia Tech. There he worked as a graduate teaching assistant for the Electrical Engineering department. He later became a graduate research assistant for the Center for Wireless Telecommunications research group. Mark will receive his Master of Science degree in Electrical Engineering in December 2001.

Since January 2000, Mark has worked as an RF Engineer for Motorola in Rolling Meadows, Illinois. He currently lives there with his wife, Christi, and his son, Allan.